

Research Article

On the Use of Gini Coefficient for Measuring Time-Frequency Distribution Concentration and Parameters Selection

Irena Orović ^{1,2}, Srdjan Stanković ² and Marko Beko ^{1,3}

¹COPELABS, Universidade Lusófona, 1700-097 Lisboa, Portugal

²University of Montenegro, Faculty of Electrical Engineering, Podgorica 81000, Montenegro

³Instituto de Telecomunicações, Instituto Superior Técnico, University of Lisbon, 1649-004 Lisboa, Portugal

Correspondence should be addressed to Irena Orović; irenao@ac.me

Received 14 September 2021; Revised 26 February 2022; Accepted 20 August 2022; Published 18 October 2022

Academic Editor: Dragan Pamučar

Copyright © 2022 Irena Orović et al. This is an open access article distributed under the Creative Commons Attribution License, which permits unrestricted use, distribution, and reproduction in any medium, provided the original work is properly cited.

The energy concentration in the time-frequency analysis has been used as an important feature in many signal processing tasks such as detection, reconstruction, feature extraction, and classification, especially in applications with nonstationary signals. Consequently, when considering the energy concentration as a feature, it is of great importance to provide the time-frequency representation that provides the highest possible concentration for a certain signal type. Measuring time-frequency distribution concentration allows an appropriate selection of distribution parameters that mostly correspond to the analyzed signal. Different types of concentration measures have been applied for automatic parameters set up in time-frequency based signal analysers. Here, we propose to use the Gini coefficient as an efficient concentration measure for an appropriate choice of time-frequency distribution and its parameters. It is proven that the Gini coefficient can be more suitable than other commonly used measures. The advantage of using the Gini coefficient is demonstrated in examples.

1. Introduction

Time-frequency representations have been widely used in the analysis of nonstationary signals, particularly the signals with time-varying spectra. The time-frequency perspective brings more information about the signal characteristics and spectral components behaviour [1]. Particularly, the time-frequency analysis reveals the energy concentration in a certain frequency band at a certain time point. However, there is no single time-frequency representation that can fit to all kinds of signals, and therefore, many different forms of time-frequency distributions have been proposed over the time [1–6]. The choice of the time-frequency distribution depends on the nature of the observed process, the number of spectral components, the rate and law of the instantaneous frequency (IF) change, etc. An appropriate time-frequency distribution will provide the highest possible energy concentration in the time-frequency domain. For signals in the real application, it is still a challenge to select an appropriate distribution among the existing choices, unless

we are well aware of the signal characteristics, but even then it is difficult to set the parameters of the chosen distribution to comply with the expected signal parameters. Consequently, significant research efforts have been focused toward the design of procedures for automated time-frequency distribution selection that would facilitate the analysis of signals in practice [3, 6]. Certainly, the most effective solutions are based on the use of concentration measures, such as the ℓ_1 -norm that has been currently widely explored in the area of compressing sensing [7]. In time-frequency analysis, a very popular measure has been introduced by Jones and Parks [8]. Here, we propose to use the Gini coefficient-based measure of time-frequency concentration, showing that it is a more reliable indicator than the commonly used measures [7–10]. The Gini coefficient outperforms these common measures concerning the time-frequency signal analysis in important scenarios described in this work.

It is interesting to mention that the use of the Gini coefficient has been also successfully explored in other interesting signal processing applications. For instance, in [11],

the authors employed the Gini coefficient in compressive sensing to provide an efficient measure of the signal's sparsity. Particularly, the Gini coefficient has been incorporated into a stochastic optimization algorithm to provide more accurate reconstruction from compressive samples. Another example is the use of the Gini index in compressive sensing ISAR imaging [12] providing high-quality image reconstruction under strong clutter and a very limited number of measurements. The improvements (over many state-of-the-art methods) achieved by using the Gini coefficient-based indexes in feature extraction methods have been proven in the application of machinery fault feature extraction [13]. The use of the Gini coefficient was also proposed in biomedical signal processing, for measuring the inequality of the power spectral density of RR intervals in ECG signals in order to use it as a psychophysiological indicator of mental stress [14], as well as for measuring the inequality in EEG waves for an efficient depth of consciousness monitoring [15].

The paper is organized as follows. In Section 2, an overview of time-frequency analysis including the commonly used time-frequency distributions is provided. Section 3 presents the most often used time-frequency concentration measures and also introduces the Gini coefficient in the time-frequency analysis. The experimental evaluation of the proposed time-frequency concentration metrics including the discussion of results is provided in Section 4, while concluding remarks are given in Section 5.

2. Theoretical Background—Time-Frequency Analysis

In this section, we provide an overview of different time-frequency distributions.

The simplest time-frequency representation is obtained using a windowed short-time Fourier transform (with s being a signal, w being a window, n and k are discrete time and frequency variables, respectively).

$$STFT(n, k) = \sum_{m=-N/2}^{N/2-1} s(n+m)w(m)e^{-j2\pi mk/N}, \quad (1)$$

whose squared absolute value is known as the spectrogram. The spectrogram is characterized by a generally low time-frequency resolution and concentration. The improved concentration is achieved using the Wigner distribution.

$$WD(n, k) = 2 \sum_{m=-N}^{N-1} s(n+m)s^*(n-m)e^{-j4\pi mk/N}, \quad (2)$$

which again has its own drawback coming from the quadratic nature and the presence of cross-term. In practical applications, the modified Wigner distribution, i.e., the S-method has been commonly used since it eliminates the cross-terms from the time-frequency domain and allows much simpler implementation. It is defined as [16]

$$\begin{aligned} SM(n, k) &= \sum_{i=-L}^L P(i)STFT(n, k+i)STFT^*(n, k-i) \\ &= |STFT(n, k)|^2 + 2\text{Re} \left[\sum_{i=1}^L P(i)STFT(n, k+i)STFT^*(n, k-i) \right], \end{aligned} \quad (3)$$

where $P(i)$ is the frequency window of length $2L+1$. It is interesting to observe that the concentration in the time-frequency domain is enhanced by increasing the value of parameter L , but the calculation complexity increases as well.

In the case when the signal's phase function varies fast, the higher-order distributions need to be considered. An appropriate choice can be the complex-lag time-frequency distribution defined as [17, 18]

$$CTD_4(n, k) = \sum_{m=-N/2}^{N/2} s(n+m)s^*(n-m)s^j(n-jm)s^{-j}(n+jm)e^{-j2\pi/N4mk}. \quad (4)$$

By analogy with the implementation of the S-method given by (3), the L-form of distributions can further improve the concentration when necessary. For instance, the L-form of the $CTD_4(n, k)$ is given by [17]

$$CTD_4^L(n, k) = \sum_{i=-N}^N P(i)CTD_4^{L/2}(n, k+i)CTD_4^{L/2}(n, k-i). \quad (5)$$

3. Measuring Concentration in the Time-Frequency Domain

One of the commonly used measures of sparsity is known as the ℓ_0 -norm defined as a number of nonzero elements (K) in a certain vector:

$$\|s\|_0 = \lim_{p \rightarrow 0} \|s\|_p^p = \lim_{p \rightarrow 0} \sum_{n=1}^N |s(n)|^p = \sum_{n=1; s(n) \neq 0}^N 1 = K. \quad (6)$$

In practical applications especially when the noise is present, the ℓ_0 -norm is commonly replaced by the ℓ_1 -norm:

$$\ell_1 = \sum_{n=1}^N |s(n)|. \quad (7)$$

The most commonly used time-frequency concentration measure was introduced in the following equation:

$$M_{JP} = \left(\frac{L_4}{L_2} \right)^4 = \frac{\sum_n \sum_k TFD^4(n, k)}{(\sum_n \sum_k TFD^2(n, k))^2}. \quad (8)$$

It represents the fourth power of the ratio of L_4 and L_2 norms of $TFD(n, k)$, where TFD represents the considered time-frequency distribution. High values of M_{JP} indicate that the distribution $TFD(n, k)$ is highly concentrated, and vice versa [6]. In the case of signals with multiple components, this measure will favour distribution that provides a high concentration of certain components although the other components may be low concentrated. An alternative measure definition in such cases can be given as follows [6]:

$$M_p^p = \left(\sum_n \sum_k |TFD(n, k)|^{1/p} \right)^p. \quad (9)$$

3.1. Using Gini Coefficient in the Time-Frequency Analysis.

In the sequel, we propose using the Gini coefficient to indicate the appropriateness of time-frequency representation for a certain signal type. For a given set of representation elements R and its sorted version R_s : $|R_s(1)| \leq \dots \leq |R_s(N)|$, the Gini coefficient can be defined as

$$G(R) = 1 - \frac{2}{\|R\|_1} \sum_{i=1}^N |R_s(i)| \left(\frac{N-i+1/2}{N} \right). \quad (10)$$

Note that the vector of representation elements R is obtained as a vector of values in the time-frequency plane captured at the specific time instant (windowed signal spectrum for an arbitrary time instant).

It is observed as a statistical measure of distribution inequality, which is scale-invariant and independent on the size of R . Gini coefficient ranges from 0 to 1: 0 means total equality, while 1 indicates total inequality. As such, it can be more suitable for concentration measurement than the common measures. For example, the two vectors $\mathbf{a} = [1, 1, 1, 1, 1, 1, 1, 1, 1, 1]$ and $\mathbf{b} = [0, 0, 0, 1, 1, 8, 1, 1, 0, 0]$ have equal ℓ_1 and ℓ_2 norms: $\|\mathbf{a}\|_{\ell_1} = \|\mathbf{b}\|_{\ell_1} = 12$, $\|\mathbf{a}\|_{\ell_2} = \|\mathbf{b}\|_{\ell_2} = 3.46$, although \mathbf{a} is spread and \mathbf{b} is highly concentrated around the central value 8. On the other hand, $G(\mathbf{a}) = 0$ indicates the equal distribution of elements in \mathbf{a} , while $G(\mathbf{b}) = 0.86$ (close to 1) indicates a high concentration at a certain element in \mathbf{b} . In that sense, the Gini coefficient can be used to choose the most concentrated time-frequency representation especially for signals exhibiting complex and nonlinear behaviour in the time-frequency domain. Moreover, as it will be proved by the examples, it can be used as an efficient metrics to set the parameters values of the time-frequency distribution that best fit to the observed signal.

4. Measuring Time-Frequency Distribution Concentration

4.1. Measuring Concentration for Different Values of Distribution Parameters. Let us observe the signal in the form:

$$s(n) = e^{j(\sin(2\pi n) + \cos(2\pi n) + \sin(3\pi n))}. \quad (11)$$

The S-method is considered as the time-frequency representation. The parameters of the signal are given as follows. The observed time interval of the signal is given by $n = -1 + T/N$: $T/N: 1$, where $T=2$, while the number of samples is $N=128$. The Hanning window is assumed with $M=128$ points which is also the size of STFT, i.e., DFT of the windowed signal part (with $M-1$ overlapping between the consecutive windows).

In order to demonstrate the efficiency of the Gini coefficient in depicting the concentration in the time-frequency domain, we have analyzed different values of parameter L in the calculation of the S-method given by (3). In Figure 1, the S-method is shown for $L=4$, $L=8$, $L=16$, and $L=24$ (left column). In order to show clearly how the concentration increases with L , the plot over a single time instant (all frequencies are included) is shown in Figure 1—right column for different values of L . By increasing the parameter L , the concentration increases, and the value of Gini coefficient increases as well. At the same time, we intend to demonstrate that the values of commonly used measures such as the measure M_{JP} defined by (8) or the ℓ_1 -norm do not follow properly this improvement in concentration. Therefore, in Table 1, we present the values of M_{JP} and ℓ_1 -norm and Gini coefficient. Note that Gini coefficient is calculated over the entire time-frequency plane (TFP) as an average value of Gini coefficients calculated for vectors at different time instants, or even using a single arbitrary chosen time instant (TFL). The measure of concentration should increase by increasing L , which is not the case when observing M_{JP} . On the other side, we may observe that the ℓ_1 -norm constantly increases with L , while in fact it should decrease. Finally, applying the Gini coefficients over the TFP and TFL can depict properly the change in concentration, since both Gini coefficient-based measures increase with L . Note that the upwards arrow indicates concentration increasing, while the downwards arrow indicates the concentration decreasing. Also, the green colour of arrow indicates the expected behaviour or the correct indication, while the red colour indicates the wrong behaviour of the considered measure. This particularly means that only the Gini coefficient-based measure shows the expected behaviour with the increase of parameter L .

From Table 1, we can also observe that the concentration measured by Gini coefficient (particularly when observing the values of Gini cf.—TFP) does not change significantly for $L > 16$, and thus, the value $L=16$ can be selected as an optimal choice of parameter for the calculation of the S-method. Note that higher L requires higher calculation complexity, so we need to select the lowest possible L providing high concentration in the time-frequency domain.

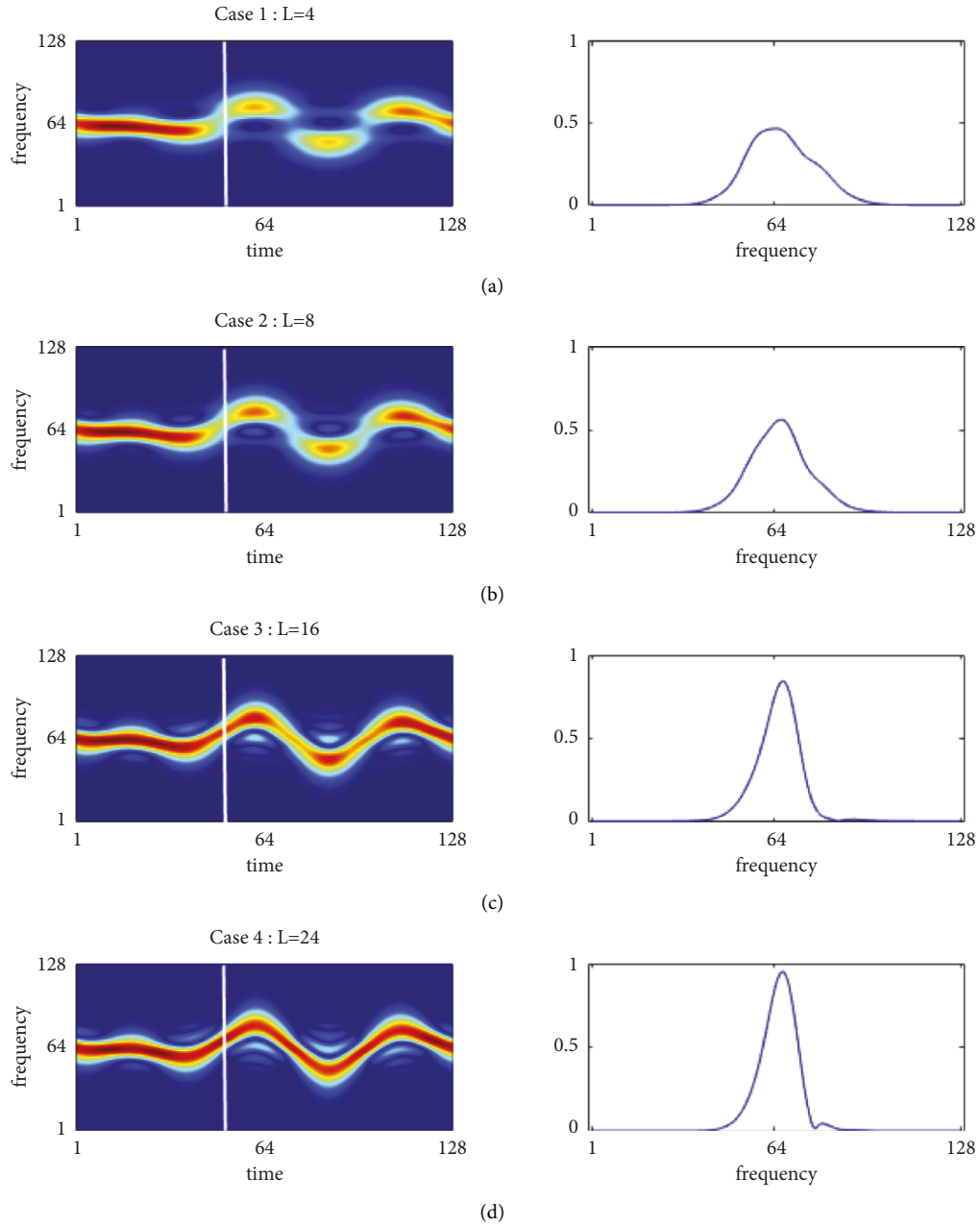


FIGURE 1: S-method for different values of parameter (L): (a) SM for $L = 4$ (left), SM at single time instant for $L = 4$ (right), (b) SM for $L = 8$ (left), SM at single time instant for $L = 8$ (right); (c) SM for $L = 16$ (left); SM at single time instant for $L = 16$ (right), (d) SM for $L = 24$ (left), SM at single time instant for $L = 24$ (right). The selected time instant depicted in the right part is marked using the white line in the left part of the figure.

TABLE 1: Different concentration measures calculated for the S-method with different values of parameter L .

L	Concentration Measures				
	M_{JP}	ℓ_1 -norm	Ginif. - TFP		Ginif. - TFL
Case 1: $L=4$	5.21 ●	$1.71 \cdot 10^3$ ●	0.78 ●		0.72 ●
Case 2: $L=8$	5.17 ↓	$1.74 \cdot 10^3$ ↑	0.80 ↑		0.75 ↑
Case 3: $L=16$	4.95 ↓	$1.88 \cdot 10^3$ ↑	0.82 ↑		0.83 ↑
Case 4: $L=24$	5.02 ↑	$1.90 \cdot 10^3$ ↑	0.828 ↑		0.85 ↑

The computation complexity of the Gini coefficient calculation is of the same order as the calculation of the ℓ_1 -norm which is $O(N)$ (N is the number of elements). Namely, according to (10), the vector norm $\|R\|_1$ is outside the summation with complexity $O(N)$, and the computation of the sum is also of order $O(N)$. In the case of M_{JP} given by (8), the calculation complexity is $O(N^2)$ for a square matrix of time-frequency representation as it is the case in the considered example.

4.1.1. Influence of Noise on the Gini Coefficient. Let us further analyse the influence of noise on the values of Gini coefficient as a measure of time-frequency concentration. Different values of SNR are observed (the noise is added to the signal in (11)), and the Gini coefficient is calculated for the S-method and $L = 16$. The results are depicted in Figure 2. Note that the Gini coefficient for the nonnoisy signal case and $L = 16$ is 0.82 (as reported in Table 1). It can be observed from Figure 2 that the value of Gini coefficient does not change significantly in the presence of noise and increases quite slowly with the increase of the noise amount, still being close to the nonnoisy case.

4.2. Gini Coefficient as a Measure of Concentration for Multicomponent Signals (Real-World Signals). Next, we observe the application of Gini coefficient as a concentration measure in optimal parameter selection for time-frequency representation of multicomponent signals. In that sense, an example with real-world signal is considered, namely real radar data containing captured multiple simultaneous human physical movements. Note that various body parts have different shifts, since they are moving with various velocities. The strongest component corresponds to the main body movements, while the other components correspond to swinging arms and other body parts. For instance, the swinging arms induce frequency modulation of the returned signal and generate side-bands about the body doppler.

The time-frequency representation is obtained by using the S-method due to the multicomponent nature of the analyzed signal. The length of the signal is 2048 samples, while the length of the applied window is 256 samples (Gaussian window is used).

Due to the complexity of the considered multicomponent signal, the selection of the convolution parameter L defining the size of the convolution window is important in the calculation of an appropriate time-frequency representation. In Figure 3, we present the S-method calculated for different values of parameter L , namely $L = \{0, 1, 2, 3, 4, 5\}$. Next, we measure the concentration measure using the Gini coefficient for each considered case. The obtained results are reported in Table 2. It can be observed that the concentration of components increases with L , achieving the maximum for $L=3$. For higher L , the cross-terms appear between the auto-components of multicomponent signal, which is an undesirable effect that degrades the time-frequency representation.

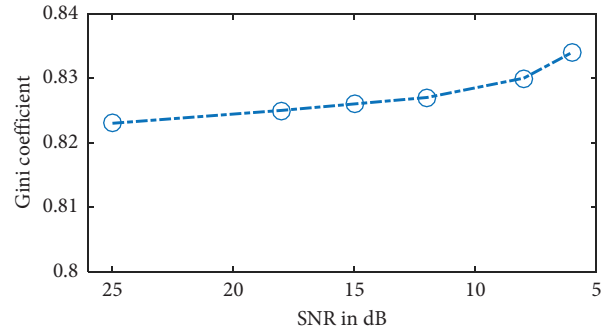


FIGURE 2: Gini coefficient calculated for S-method and $L = 16$ for different values of SNR.

4.3. Algorithm: Optimal Parameter Selection for TF Representation. According to the previous analyses, we can employ Gini coefficient for optimal parameter selection, but it is necessary to distinguish the case of monocomponent and multicomponent signals. In the case of monocomponent signals, the concentration will constantly increase with the increase of parameter L in the case of the S-method. After a certain value of L , the concentration improvement will not be significant anymore, and the algorithm can stop the procedure of increasing L . On the other hand, in the case of multicomponent signals, although the concentration of auto-components will increase with L as in the case of monocomponent signals, the cross-terms appear for a certain value of L as a consequence of convolving different auto-components. The Gini coefficient as a concentration measure will achieve a maximum for the largest value of L that does not produce cross-terms. Therefore, a simple algorithm for optimal parameter selection in the case of the S-method is provided in the sequel. (Algorithm 1)

Having in mind that the Gini coefficient takes values between 0 and 1, the value of tolerance parameter δ for monocomponent can be set to 0.01 for the type of signals consider in the examples. However, for other types of signals and applications, it can be determined empirically.

4.4. Comparing the Concentration between Different Types of Distributions. The signal considered in this example is characterized by faster instantaneous frequency variations compared to the previous example. Such time-varying components usually appear in radar applications and correspond to the microdoppler components bringing useful information about the fast-moving target parts. Note that these signals are commonly modeled by using sine (cosine)-modulated phase terms: $s(n) = e^{j(A_k \sin(a_k \pi n) + B_l \cos(b_l \pi n))}$, $k = 1, \dots, K$, and $l = 1, \dots, L$.

For instance, let us observe an example of the signal in the form:

$$s(n) = e^{j(2 \sin(2\pi n) + \sin(3\pi n) + \cos(3\pi n))}, \quad (12)$$

where the signal parameters and window length are assumed as in the case of signal given by (11).

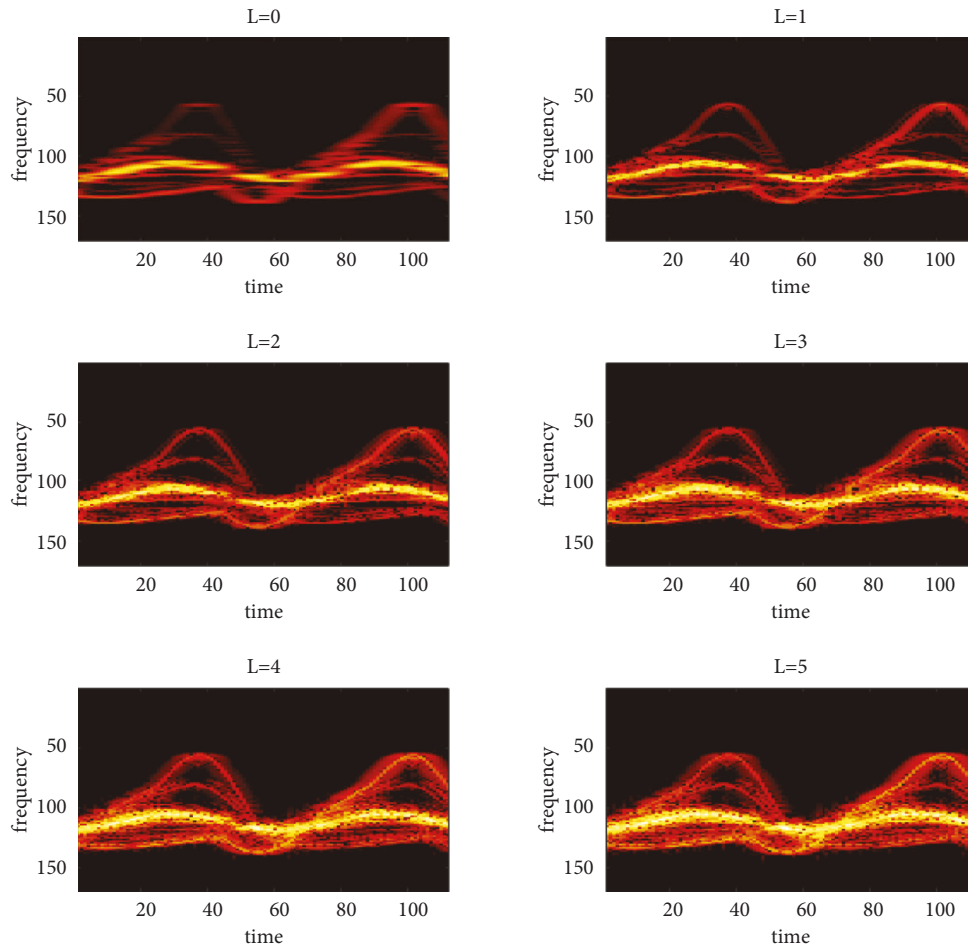


FIGURE 3: S-method calculated for real radar data, considering different values of parameter L , i.e., $L = \{0, 1, 2, 3, 4, 5\}$.

TABLE 2: Gini coefficient calculated for the S-method of real radar data for different values of parameter L .

L	Concentration measure Gini cf.
Case 1: $L = 0$	40.02
Case 2: $L = 1$	61.15
Case 3: $L = 2$	67.36
Case 4: $L = 3$	68.18
Case 5: $L = 4$	64.79
Case 6: $L = 5$	62.09

Due to the fast-varying spectral behaviour, it is necessary to use higher-order time-frequency distribution in order to provide highly concentrated representation. Therefore, we observe three different time-frequency distributions: (a) the S-method, (b) the complex-lag distribution (CTD), and (c) L-form of the CTD. The aim is to show that the Gini coefficient can provide more accurate estimate of the distribution concentration compared to the measure M_{JP} . The considered time-frequency distributions are shown in the left column of Figure 4, while the right column shows the frequency contents along one arbitrary time instant (vertical slice of TFD). The Gini coefficient and the measure M_{JP} are reported in Table 2 for each considered case. The S-method (Figure 4(a)) is calculated for larger L

($L = 16$ is used to provide better concentration). The CTD is affected by the innerinterference terms that ruin the concentration (Figure 4(b)). Namely, the spectral components are spread along all frequencies, which is reflected in the lower value of the Gini coefficient (Table 3) compared to the SM. However, the value of measure M_{JP} for CTD increases unduly.

Finally, the concentration measures are the highest in the case of LCTD, where again the Gini coefficient brings more meaningful information: the value 0.9 is close to the maximal value 1 representing an ideally concentrated peak and consequently the preferred distribution choice. On the other hand, the values M_{JP} in its absolute amounts do not provide clear information about the concentration itself [16–18].

```

Input: signal
Set:  $L = 1$ 
Case 1: multicomponent signal
  if  $TFP(SM(L)) > TFP(SM(L-1))$  % $TFP(SM(L))$  is average Gini coefficient for S-method and chosen  $L$ 
     $L = L + 1$ ;
  else
    break;
  end
Case 2: monocomponent signal
  if  $TFP(SM(L)) - TFP(SM(L/2)) > \delta$ 
     $L = 2 * L$ ;
  else
    break;
  end
Output:  $L, SM(L)$ 
    
```

ALGORITHM 1: Optimal parameter selection in the S-method calculation.

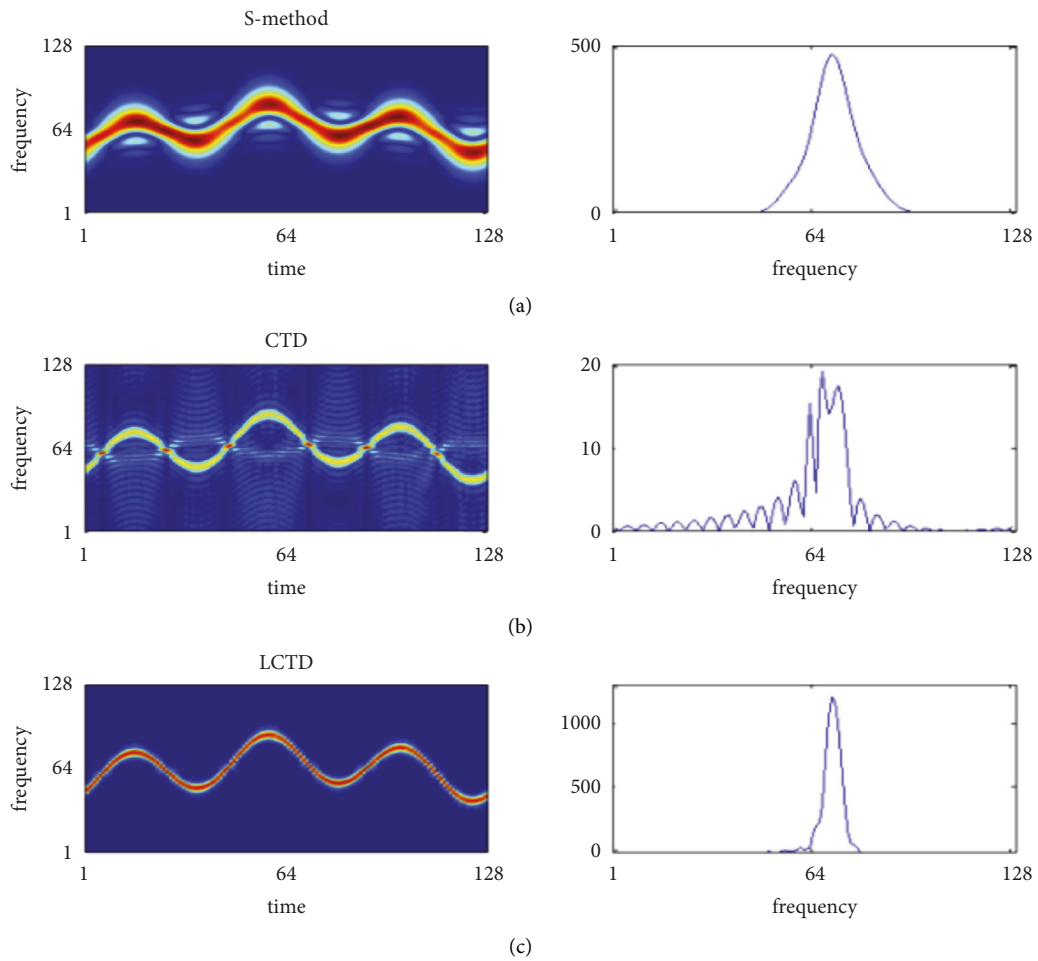


FIGURE 4: (a) SM (left) and plot of its single time instant (right), (b) CTD (left) and plot of its single time instant (right), (c) LCTD (left) and plot of its single time instant (right).

TABLE 3: Concentration measures for different TF distributions.

Distribution	Concentration measures	
	M_{JP}	Gini cf.—TFP
SM	4.39	0.79
CTD	6.94	0.58
LCTD	14.13	0.90

5. Conclusions

Improving the energy concentration in the time-frequency domain and reducing the spectral leakage have been the focus of research interests for signal processing and feature selection applications. In order to ease and unify the process of selecting an appropriate form of time-frequency distribution that can provide a satisfactory level of energy concentration, this work proposes the application of Gini coefficient-based metric for quantifying the concentration in the time-frequency domain. The efficient performance of this measure is demonstrated in two important scenarios, namely, the selection of time-frequency distribution parameters as shown in the case of the S-method, as well as in the comparison of different time-frequency distributions. The results have shown that the Gini coefficient provides more meaningful results comparing to the commonly used time-frequency measures. The proposed approach provides an efficient engineering tool in designing the procedures for automated time-frequency distribution selection that can facilitate the analysis of nonstationary signals in practice.

Data Availability

Data sharing not applicable to this article as no datasets were generated or analyzed during the current study.

Conflicts of Interest

The authors declare that they have no conflicts of interest.

Acknowledgments

This research was partially funded by the Fundação para a Ciência e a Tecnologia under Projects UIDB/04111/2020, ROBUST EXPL/EEI-EEE/0776/2021, and CEECIND/01830/2018.

References

- [1] L. Cohen, *Time-Frequency Analysis: Theory and Applications*, Prentice Hall PTR, Englewood Cliffs, NJ, 1995.
- [2] P. Flandrin, R. G. Baraniuk, and O. Michel, "Time-frequency complexity and information," *Proc. ICASSP*, vol. 3, pp. 329–332, 1994.
- [3] I. Orović, M. Orlandić, S. Stanković, and Z. Uskoković, "A virtual instrument for time-frequency analysis of signals with highly non-stationary instantaneous frequency," *IEEE Transactions on Instrumentation and Measurement*, vol. 60, no. 3, pp. 791–803, 2011.
- [4] E. Sejdić, I. Djurović, and J. Jiang, "Time-frequency feature representation using energy concentration: an overview of recent advances," *Digital Signal Processing*, vol. 19, no. 1, pp. 153–183, 2009.
- [5] J. Lerga and V. Sucić, "Nonlinear IF estimation based on the PseudoWVD adapted using the improved sliding pairwise ICI rule," *IEEE Signal Processing Letters*, vol. 16, no. 11, pp. 953–956, 2009.
- [6] L. Stanković, "A measure of some time-frequency distributions concentration," *Signal Processing*, vol. 81, no. 3, pp. 621–631, 2001.
- [7] D. Donoho, "Compressed sensing," *IEEE Transactions on Information Theory*, vol. 52, no. 4, pp. 1289–1306, 2006.
- [8] D. L. Jones and T. W. Parks, "A high resolution data-adaptive time-frequency representation," *IEEE Transactions on Acoustics, Speech, & Signal Processing*, vol. 38, no. 12, pp. 2127–2135, 1990.
- [9] I. Shafi, J. Ahmad, S. I. Shah, and F. M. Kashif, *Quantitative Evaluation of Concentrated Time-Frequency Distributions*, EUSIPCO, Glasgow, Scotland, 2009.
- [10] D. Malnar, V. Sucić, and J. M. O'Toole, "Automatic quality assessment and optimisation of quadratic time-frequency representations," *Electronics Letters*, vol. 51, no. 13, pp. 1029–1031, 2015.
- [11] D. Zonoobi, A. A. Kassim, and Y. V. Venkatesh, "Gini index as sparsity measure for signal reconstruction from compressive samples," *IEEE Journal of Selected Topics in Signal Processing*, vol. 5, no. 5, pp. 927–932, 2011.
- [12] C. Feng, L. Xiao, and Z. H. Wei, "Compressive sensing inverse synthetic aperture radar imaging based on Gini index regularization," *International Journal of Automation and Computing*, vol. 11, no. 4, pp. 441–448, 2014.
- [13] Y. Miao, J. Wang, B. Zhang, and H. Li, "Practical framework of Gini index in the application of machinery fault feature extraction," *Mechanical Systems and Signal Processing*, vol. 165, Article ID 108333, 2022.
- [14] M. E. Sánchez-Hechavarría, S. Ghiya, R. Carrazana-Escalona et al., "Introduction of application of Gini coefficient to heart rate variability spectrum for mental stress evaluation," *Arquivos Brasileiros de Cardiologia*, vol. 113, no. 4, pp. 725–733, 2019.
- [15] K. J. You, G. J. Noh, and H. C. Shin, "Spectral Gini index for quantifying the depth of consciousness," *Computational Intelligence and Neuroscience*, vol. 2016, pp. 1–12, 2016.
- [16] L. Stanković, "A method for time-frequency analysis," *IEEE Transactions on Signal Processing*, vol. 42, no. 1, pp. 225–229, 1994.
- [17] S. Stanković, I. Orović, and C. Ioana, "Effects of cauchy integral formula discretization on the precision of IF estimation: unified approach to complex-lag distribution and its L-form," *IEEE Signal Processing Letters*, vol. 16, no. 4, pp. 307–310, 2009.
- [18] S. Stanković, N. Zaric, I. Orović, and C. Ioana, "General form of time-frequency distribution with complex-lag argument," *Electronics Letters*, vol. 44, no. 11, pp. 699–701, 2008.